

Cite this: *Food Funct.*, 2022, **13**, 2631

The protective effect of C-phycocyanin in male mouse reproductive system

 Fang-Hao Yang,^a Xiao-Lei Dong,^a Guo-Xiang Liu,^a Lei Teng,^a Lin Wang,^b Feng Zhu,^a Feng-Hua Xu,^a Yi-Fan Yang,^a Can Cao,^a Guang Chen^a and Bing Li *^{a,c}

C-phycocyanin from *Spirulina platensis* has pharmacological effects such as anti-oxidation, anti-cancer, anti-inflammatory and anti-atherosclerosis activities as well as liver and kidney protection. However, there is little research on C-phycocyanin applied in the field of reproductive medicine, and it is therefore the focus of the current study. In this study, a GC-1 spg cell model and male mouse reproductive injury model were constructed by TNF α + Smac mimetic + zVAD-fmk (TSZ) and cyclophosphamide (Cy), respectively. It has been proved that C-phycocyanin can increase cell viability and reduce cell death in GC-1 spg cells induced by TSZ. C-phycocyanin could protect the reproductive system of male mice from cyclophosphamide, improve spermatogenesis, sperm quality and fertility, increase the release of testosterone, stabilize the feedback regulation mechanism, and ensure the spermatogenic ability of mice. It could also improve the ability of anti-oxidation. In addition, C-phycocyanin could play a protective role by down-regulating RIPK1, RIPK3, and p-MLKL to inhibit the necroptotic signaling pathway. These results suggest that C-phycocyanin could protect GC-1 spg cells and the reproductive system of male mice from TSZ and cyclophosphamide, and the protective mechanism may be achieved by inhibiting the signal pathway of necroptosis. Therefore, C-phycocyanin could serve as a promising reproductive system protective agent. C-phycocyanin may enter public life as a health product in the future.

Received 5th November 2021
Accepted 27th January 2022

DOI: 10.1039/d1fo03741b

rsc.li/food-function

1. Introduction

At present, male infertility and reproductive dysfunctions have become major global health problems.¹ Globally, about 10% to 15% of couples are affected by various conditions that lead to infertility, with up to 50% of those affected by male factors.^{1,2} More than 30 million people worldwide suffer from male infertility.³ Male infertility not only causes psychological pain to families but also increases certain economic burdens faced by society.^{4,5} In a prospective study on Danish men, it was found that infertile men died at a higher rate than those who were fertile.⁶ Many congenital and acquired causes and risk factors contribute to male reproductive health.^{7,8} Male oxidative stress infertility mainly involves changes in semen characteristics in men affected by environmental or occu-

pational exposure to toxic chemicals and various lifestyle factors.^{9,10} The use of certain chemotherapy drugs can also cause male infertility.¹¹

Cyclophosphamide (Cy) is a broad-spectrum antitumor drug used for the chemotherapy of many tumors, but its toxicity and side effects on the reproductive system are huge, such as gonad damage.¹² In the prenatal stage, cyclophosphamide has harmful effects on the male reproductive system, resulting in decreased testicular weight and sperm count, and increased abnormalities of the sperm head, neck, and tail.^{13,14} In addition, studies have shown that antioxidant treatment before chemotherapy can reduce the damage caused by cyclophosphamide to the gonads, and has ameliorated cyclophosphamide-induced injury through modulation of the expression of genes contributing to the function of Sertoli and spermatogenic cells.¹⁵

C-phycocyanin (C-PC) is a protein-binding pigment found in cyanobacteria. It is a polymer composed of two distinguishable protein subunits, α and β , which contain at least three covalently attached bilin choline chromophores. C-phycocyanin is the most abundant pigment in cyanobacteria, with good water solubility and spontaneous red fluorescence.^{16–18} A number of pharmacological studies have demonstrated that C-phycocyanin has a variety of functions, such as anti-oxidant,¹⁹ anti-tumor,²⁰ anti-inflammatory²¹ and anti-athero-

^aDepartment of genetics and cell biology, Basic medical college, Qingdao University, Qingdao, China, 266071. E-mail: yfhao1996@163.com, dongxiaoleiqd@163.com, 13869845003@163.com, qtlei@sina.com, sedolphin@163.com, 1697891180@qq.com, zhuchengyangyifan@163.com, 2505217841@qq.com, 602252921@qq.com

^bDepartment of Reproduction, The Affiliated Hospital of Qingdao University, Qingdao, China, 266000. E-mail: wanglincyf@126.com

^cDepartment of hematology, The Affiliated Hospital of Qingdao University, Qingdao, China, 266021. E-mail: libing_516@qdu.edu.cn; Tel: +86-532-82991029

sclerosis.²² In recent years, C-phycoyanin has become a hot research spot in reproductive medicine. C-phycoyanin was proved to improve fertility by improving ovary and oocyte quality in obese female mice.²³ C-phycoyanin has beneficial effects on the development of porcine parthenotes by attenuating mitochondrial dysfunction and oxidative stress,²⁴ and may be useful for improving porcine oocyte quality and subsequent developmental competence in embryos.²⁵

Necroptosis is a type of programmed necrotic cell death and caused by the tumor necrosis factor family of cytokines. Receptor-interacting protein kinase-1(RIPK1), receptor-interacting protein kinase-3(RIPK3) and mixed lineage kinase domain-like protein (MLKL) are three key proteins of the necroptosis pathway.^{26,27} Necroptosis is associated with a variety of disease states, such as myocardial infarction and stroke,^{28,29} atherosclerosis,³⁰ ischemia-reperfusion injury,^{31,32} pancreatitis,^{33,34} inflammatory bowel disease.^{35,36} Recent research suggests that necroptosis also plays a role in the development of the reproductive system. RIPK3 and MLKL knockout mice retain 'youthful' morphology and function into advanced age, while those of age-matched wild-type mice deteriorate. Feeding RIPK1 inhibitors to wild-type mice effectively prevented the appearance of signs of aging.³⁷ RIPA-56, a RIPK1 inhibitor that can inhibit necroptosis, could be a novel agent to preserve fertility in male mice with busulfan-induced gonadotoxicity.³⁸ Otherwise, p-MLKL may potentially serve as a seminal biomarker for the spermatogenic function in men. Necroptosis occurs more frequently in the aging human testes with regressive spermatogenic function. The expression of p-MLKL in seminal plasma was negatively related to sperm concentration and would raise in advance on the point of testicular hypofunction.³⁹

In our study, we investigated the role of C-phycoyanin in the development of the male mouse reproductive system. C-phycoyanin can protect GC-1 spg cells from TSZ damage, improve proliferation ability and reduce the death of GC-1 spg cells. In addition, we also detected the expression of molecules related to necroptosis and found that C-phycoyanin can reduce the expression of TNF- α , RIPK1, RIPK3, p-MLKL. Moreover, animal experiments also showed that C-phycoyanin could improve spermatogenesis in male mice, and protect the normal development of the reproductive system, while also reducing the expression of key molecules related to necroptosis in testicular tissue. Therefore, through the analysis of the above experimental results, C-phycoyanin could play a certain protective role in the reproductive system by inhibiting the occurrence of reproductive cell death.

2. Materials and methods

2.1 Chemical reagents

C-phycoyanin was purchased from Binmei Biotechnology (Taizhou, China). Cell Counting kit-8 (CCK-8) was purchased from Biosharp, Hefei, China. Cyclophosphamide monohydrate (C₇H₁₅Cl₂N₂O₂P·H₂O, C106991, China), Necroptosis Inducer

Kit with TSZ (C1058S, China), Necrostatin-1 (TNF-alpha inhibitor) (SC4359-25 mg, China), Annexin V-FITC/PI Apoptosis Detection Kit (40302ES60, China), eBioscience™ Annexin V Apoptosis Detection Kit APC (88-8007-72, USA), Mouse T ELISA Kit (ml001948, China), Mouse FSH ELISA Kit (ml001910, China), Mouse LH ELISA Kit (ml063366, China), an antibody against Phospho-MLKL (Ser358, AF7402), and antibody against TNF-alpha (AF7014) were from Affinity (China). The antibody against RIPK1 (A7414), antibody against MLKL (A131451), antibody against RIPK3 (A5431), antibody against Caspase-8 (A0215), FITC Goat Anti-Rabbit IgG (H + L) (AS011) were from ABclonal (China). Countess™ cell counting chamber slides were purchased from Invitrogen by Thermo Fisher Science.

2.2 Cell culture

GC-1 spg cell, a spermatogonial cell line, was purchased from Procell Life Science&Technology Co., Ltd (Wuhan, China). GC-1 spg cell was cultured in high glucose DMEM (Biological Industries, Israel) supplemented with 10% fetal bovine serum (Biological Industries, Israel), 100 U ml⁻¹ streptomycins and 100 U ml⁻¹ penicillin in a humidified incubator with 5% CO₂/95% air atmosphere at 37 °C.

2.3 Cell viability assay

The cell viability of GC-1 spg cell was detected by the CCK8 assay. GC-1 spg cells (8000 cells per well) were plated into 96-well cell culture plates for 12 h. Then, the medium was replaced with fresh medium with various concentrations of C-phycoyanin (0, 50, 100, 200, 400, 800, 1600 $\mu\text{g ml}^{-1}$) for 12, 24, 36 or 48 h. After treatment, CCK8 was added to the medium for 2 h according to the manufacturer's instructions. Finally, the absorbance value was measured at 450 nm and the absorbance value was positively correlated with cell viability. The best concentration and time of C-phycoyanin were determined.

In the same method, GC-1 spg cells were treated with different concentrations of necroptosis inducer reagent with TSZ (TSZ, TNF α + Smac mimetic + zVAD-fmk), and CCK8 was used to determine the best concentration and time of TSZ.

After the concentration and time of C-phycoyanin and TSZ were determined, the cells were treated with C-phycoyanin and TSZ at the same time, and then the cell viability was determined by CCK8 to determine whether C-phycoyanin could effectively inhibit the effect of TSZ on cells.

2.4 Flow cytometry

The necrotic rate of GC-1 spg cells was detected using flow cytometry. GC-1 spg cells (1 \times 10⁵ cells per well) were plated into 6-well cell culture plates for 12 h. After treatment, GC-1 spg cells were digested with trypsin without EDTA, and the cells were collected by centrifugation (300g) at 4 °C for 5 min. The cells were washed with precooled PBS 2 times, and each time was centrifuged (300g) at 4 °C for 5 min. PBS was discarded and 100 μl of 1 \times binding buffer was added to resuspend cells. Annexin V-FITC and PI staining solution were added and cells were incubated at 37 °C for 15 min in the dark. 1 \times

binding buffer was added, mixed and placed on ice. The sample was detected by flow cytometry within 1 h.

2.5 Immunofluorescence

GC-1 spg cells were cultured in 24-well cell slides. After treatment, the culture medium was sucked off and washed twice with PBS, then fixed with methanol for 15 min, and then blocked with 5% BSA for 20 min. After BSA blocking, the primary antibody and the FITC-labelled fluorescent second antibody were added respectively. Finally, it was stained with DAPI. The positive cells were observed using a fluorescence microscope and counted.

2.6 Animals and treatment

In this study, 8-week-old ICR male and female mice were purchased from Jinan Pengyue Laboratory Animal Technology (Jinan, China). The experimental animals were placed in a group with random access to water and food, five in each cage. They were maintained in a light/dark cycle for 12 hours at a stable temperature (23–25 °C) (the lights are on from 7:00 am to 7:00 pm). All animal experiments were conducted in compliance with the ethical guidelines established by the institutional ethical committee of the Qingdao University (Qingdao, China).

All the mice were randomly assigned to the control group, the Cy model group and the C-PC treatment group, then the

C-PC treatment group was divided into low (100 mg kg⁻¹ d⁻¹) and high (500 mg kg⁻¹ d⁻¹) dose groups, and the experiment was carried out according to Fig. 1.

Control group: Intra-gastric administration with water (0.2 ml), every three days one time for 10 times, injected with normal saline (NS, 0.9%) intraperitoneally, two days one time for 5 times.

Cy model group: Intra-gastric administration with water (0.2 ml), three days one time for 10 times, injected with Cy (50 mg kg⁻¹ d⁻¹) intraperitoneally, two days one time for 5 times.

Cy + C-PC (low) group: Intra-gastric administration with C-PC solution (100 mg kg⁻¹ d⁻¹), three days one time for 10 times, injected with Cy (50 mg kg⁻¹ d⁻¹) intraperitoneally, two days one time for 5 times.

Cy + C-PC (high) group: Intra-gastric administration with C-PC solution (500 mg kg⁻¹ d⁻¹), three days one time for 10 times, injected with Cy (50 mg kg⁻¹ d⁻¹) intraperitoneally, two days one time for 5 times.

In the first 30 days of the experiment, the mice in the C-PC treatment group were given different doses of C-PC solution, while the control group and Cy model group were given the same dose of water every three days, for a total of 10 times. From the 21st to the 30th day of the experiment, the mice in the Cy model group and the C-PC treatment group were intraperitoneally injected with cyclophosphamide solution, while

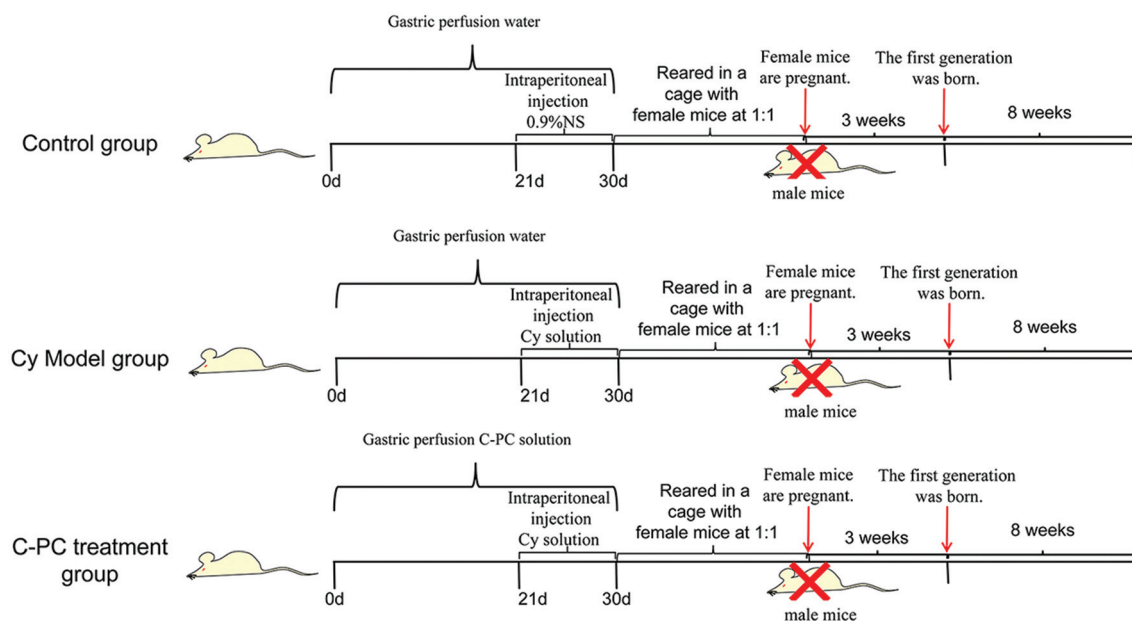


Fig. 1 The establishment of a mouse model of reproductive injury and the basic process of the design and implementation of animal experiments. (a) Three groups: control group (no processing has been carried out), Cy model group (the model of reproductive injury was established by intraperitoneal injection of cyclophosphamide solution (50 mg kg⁻¹), and intra-gastric water was given to observe the damage of the reproductive system and the response of the body in mice), C-PC treatment group (the reproductive injury model was established by intraperitoneal injection of cyclophosphamide solution, and different doses of C-PC solution were intra-gastrically administered to explore the protective effect of C-PC on cyclophosphamide-induced reproductive system injury in mice). (b) Process: the first 30 days of the experiment was the period of the construction and administration of the animal model, followed by the mating experiment until the male mice were separated after the female mice were pregnant. The pregnant female mice gave birth to offspring that were raised and allowed to grow up, and the growth and survival of the offspring were observed.

the mice in the control group were injected with the same dose of normal saline, once every two days, for a total of 5 times. After the last intragastric administration, five mice in each group were randomly selected and raised in cages with female mice at 1:1. After the female mice became pregnant, the male mice were separated from the cages for the following experiments. After the females gave birth to the offspring, the offspring were raised and grown-up and the growth and survival of the offspring were recorded.

2.7 The index of reproductive organs

When the female mice were pregnant, all-male mice were starved for 24 h, then were sacrificed. All organs were washed in normal saline solution, sucked dry with normal filters, and then weighted. Organ index = (organ mass (mg)/body mass (g)) × 100%.

2.8 Collection of blood, testis and epididymis

Before the male mice were killed, the whole blood was collected by the method of eye orbit in a 1.5 ml centrifuge tube and allowed to clot for 30 minutes at room temperature. The whole blood was centrifuged at 2000 rpm at room temperature for 15 minutes, and the serum was transferred to another centrifuge tube. It was stored at −80 °C for hormone estimation. One testis was fixed in formaldehyde (4%) for histological evaluation, and the other was stored at −80 °C for protein and RNA extraction. Sperm were collected from the tail of the epididymis. Briefly, the epididymal tail was quickly removed and cut into small pieces after euthanasia, put into 1 ml HTF culture at 37 °C to extract sperm. The released spermatozoa were collected to prepare a sperm suspension for analyzing sperm parameters.

2.9 Measurement of sperm quality levels

Sperm count: The sperm suspension (10 µl) was taken and added to the cell counting chamber slides, counted with a Countess II Automated cell counter.

Sperm deformity rate: A drop of sperm suspension and 2% eosin solution were taken on a glass slide, then covered with a cover slide. After 1 h, the sperms were observed under a light microscope at ×400 magnification. The sperm morphology was observed according to the red staining of dead sperms, and the sperm deformity rate was calculated.

Sperm mortality: 500 µl of the sperm suspension was centrifuged at 1000 rpm at room temperature for 5 min, washed with PBS and binding buffer, and the sperm concentration was $1-5 \times 10^6 \text{ ml}^{-1}$. 5 µL Annexin V-FITC was added and incubated at room temperature and hidden from light for 15 min. The sperms were washed once with the binding buffer and resuspended with 200 µl binding buffer. 3 µl of propidium iodide staining solution was added and the samples were evaluated using flow cytometry within 1 h.

2.10 Testicular homogenate analysis

Testicular tissues of 5 mice were selected for each group, and 0.1 g of tissue was converted into 10% homogenate with pre-frozen saline. Superoxide dismutase (SOD) activity and malon-

aldehyde (MDA) content were determined according to the kit's instructions (Beijing, China), and the protein content in the homogenate was detected using the BCA protein assay kit (Beyotime, China). SOD activity and MDA content were corrected by the protein concentration.

2.11 Enzyme-linked immunosorbent assay (ELISA)

The frozen serum melted slowly at 4 °C, and then the levels of serum testosterone (T), luteinizing hormone (LH) and follicle-stimulating hormone (FSH) were determined by the ELISA method according to the instructions of the kit. The optical density of the reaction solution at 450 nm was detected and the standard curve was fitted.

2.12 Testicular histopathology

The right testis and kidney were fixed in 10% neutral-buffer formalin for 72 hours to preserve the microstructure of the tissue. After the testicular and kidney section was made, HE staining was performed. The testicular and kidney histopathology were observed under a light microscope (Nikon Light ECLIPSE E200) and captured with a DXM1200 digital camera (Nikon).

2.13 Analysis of the spermatogenic dynamics

We randomly selected seminiferous tubules in 10 sections from each animal to evaluate the cell populations of the seminiferous tubule sections after HE staining. The spermatogonium, primary spermatocytes, secondary spermatocytes and spermatozoa in each seminiferous tubule were counted under a light microscope (Nikon Light ECLIPSE E200), and the spermatogenic dynamics of testis was analyzed.

2.14 Measurement of the Leydig cell volume

The testicular tissue sections of each group of mice were randomly selected and stained with HE. Under a light microscope (Nikon Light ECLIPSE E200), the nuclear diameter and cell diameter of Leydig cells were measured using the NIS elements analysis system, and then the volume of the nucleus and Leydig cell was calculated.

2.15 Immunohistochemistry

The expression of RIPK1, RIPK3 and p-MLKL in testicular tissue was detected by immunohistochemistry. The fixed testicular tissue was embedded and sliced. The slices were separated with xylene, then rehydrated into graded ethyl alcohol (100%, 95% and 75%), and then washed with tap water. Antigen retrieval was conducted by sodium citrate antigen retrieval solution (pH 9.0) in a 99 °C water bath for 30–40 min. The activity of endogenous peroxidases was blocked by a peroxidase blocker for 10 min and it was sealed with goat serum for 10 minutes. The slides were washed twice in PBS and incubated with primary antibody at 4 °C overnight. The slides were washed twice in PBS prior to their incubation as a secondary antibody for 1 h at room temperature. The slides were washed in PBS twice and incubated with DAB chromogenic fluid for 5–8 min. The following step was counterstaining using hematoxylin solution. Then, dehydration of tissues was done using

graded ethanol (75%, 95%, and 100%) and xylene. Finally, the slides were mounted using permount TM mounting medium. To make the experimental results more visible, we also carried out the corresponding quantitative analysis. Three repeated samples were collected in each group, and five fields were selected for each sample.

2.16 Quantitative real-time PCR

GC-1 spg cells were plated into 6-well cell culture plates, after treatment, the cells were collected by centrifugation, and the total RNA was extracted using TRIzol reagent (Invitrogen) according to the manufacturer's instructions. Complementary DNAs (cDNAs) were generated using the first-strand cDNA synthesis kit (abm company). The cDNA was synthesized by reverse transcription with 1 μg total RNA and random primers. Quantstudio5 real-time fluorescence quantitative PCR system was used to detect the expression level of gene mRNA. Human glyceraldehyde 3-phosphate dehydrogenase (GAPDH) was normalized as an internal reference gene. The levels of GAPDH, TNF- α , RIPK1, RIPK3 mRNA were measured by the SYBR Green assay. TNF- α was amplified by using the primers with the sequence 5'- GCCTCTTCTCATTCTGCTTGTGG-3' (forward) and 5'- GTGGTTTGTGAGTGTGAGGGTCTG -3' (reverse). The RIPK1 primer was 5'- CGACTTCCAGACACCAAGCCATC -3' (forward) and 5'- TTTCCACTGCCTTCCCAGGTTTTTC -3' (reverse). The RIPK3 primer was 5'- AAATGGATTGCCCGA-GGGAAACC -3' (forward) and 5'- AACTGATGTGCTCTGTGC-TTGCC -3' (reverse). The reaction was carried out under the following conditions: 95 $^{\circ}\text{C}$ for 30 s, 40 cycles at 95 $^{\circ}\text{C}$ for 15 s, and 60 $^{\circ}\text{C}$ for 30 s. Values of each group mRNA level were calculated as $2^{-\Delta\Delta\text{Ct}}$ levels and performed at least four times.

2.17 Western blot analysis

GC-1 spg cells were plated into 6-well cell culture plates, and after treatment, the cells were collected by centrifugation and used to extract protein. Testicular tissues of 5 mice were selected for each group, and 0.2 g of tissue was used to extract protein.

BCA protein assay kit (Beyotime Biotechnology, Shanghai, China) was used to detect the concentration of protein samples. First, 40 μg protein was mixed with SDS loading buffer (5 \times) and boiled for 10 min. Then, the protein samples were separated using 10% SDS-PAGE and transferred to the PVDF membrane (Millipore). The membrane was blocked with 5% bovine serum albumin at room temperature for 2 h and then incubated overnight with a specific primary antibody at 4 $^{\circ}\text{C}$. After washing with TBS-Tween 20 (0.1%, v/v) three times, the membrane was incubated with an appropriate HRP-secondary antibody for 1 h. After being washed with TBST three times, the blots were detected using enhanced chemiluminescence (Millipore).

2.18 Statistical analysis

Each experiment should be repeated three or four times independently. The results were expressed by mean \pm standard deviation (SD). Statistical analysis was performed by the

Student's test or one-way analysis of variance (ANOVA) by using a statistical software package (SPSS, USA). $P < 0.05$ is considered to be statistically significant.

3. Results

3.1 Effect of C-phycoerythrin on the viability of GC-1 spg cells

The effect of C-phycoerythrin on GC-1 spg cells was firstly evaluated by the CCK-8 cell viability assay. The changes of GC-1 spg cells viability were detected after the cells were treated with different concentrations of C-phycoerythrin solution for 12, 24, 36, 48 h. The results showed that cell viability was increased in a low-dose concentration solution of C-phycoerythrin ($\leq 400 \mu\text{g ml}^{-1}$), while was decreased in a high-dose concentration solution of C-phycoerythrin ($\geq 800 \mu\text{g ml}^{-1}$) in GC-1 spg cell line (Fig. 2A). From the above experimental results, the final concentration of C-phycoerythrin used in the following experiments was $100 \mu\text{g ml}^{-1}$ and the culture time was 24 h.

3.2 GC-1 spg cells were induced by necroptosis inducer kit with TSZ

The effect of TSZ on GC-1 spg cells was firstly evaluated by the CCK-8 cell viability assay. The changes of GC-1 spg cells viability were detected after the cells were treated with different concentrations of TSZ for 4, 8, and 12 h. The results showed that cell viability was reduced in a dose-dependent manner in GC-1 spg cell line (Fig. 2B). In our subsequent experiments, the treated concentration of TSZ was 2 \times . In order to further study the mechanism of TSZ-induced cell death, a series of experiments were conducted. According to the report of S. Pietkiewicz,⁴⁰ necroptotic cells can be detected after staining with Annexin V/PI by flow cytometry, the healthy, necroptotic, early and late apoptotic cell populations can be distinguished easily with their method. The necroptotic cells were detected by flow cytometry after different periods of treatment with TSZ (2 \times). The results showed that the percentage of necroptotic cells (Annexin V⁺/PI⁺) increased from 1.85%, 0.57%, 8.63%, 15.22%, to 23.98% with time (Fig. 2C). Furthermore, we carried out an immunofluorescence assay to detect the expression of p-MLKL, a key protein of necroptosis. p-MLKL-positive cells were increased gradually with time (Fig. 2D). In addition, we further detected the expression of TNF- α , RIPK1, RIPK3, and p-MLKL at the protein level. The results showed that the expression of TNF- α , RIPK1, RIPK3, and p-MLKL gradually increased with time (Fig. 2E). In conclusion, these results suggested that TSZ could induce necroptosis in GC-1 spg cells.

3.3 C-phycoerythrin can inhibit TSZ-induced necroptosis

In order to further study whether C-phycoerythrin can effectively inhibit TSZ-induced necroptosis, TSZ and C-PC were used in co-treated, and Necrostatin-1 (Nec-1), a TNF-alpha inhibitor, as the positive control. The GC-1 spg cells were treated with TSZ for 12 h, C-PC ($100 \mu\text{g ml}^{-1}$) for 24 h and Nec-1 (50 μM) for 24 h. The CCK8 assay showed that the cell viability of the TSZ

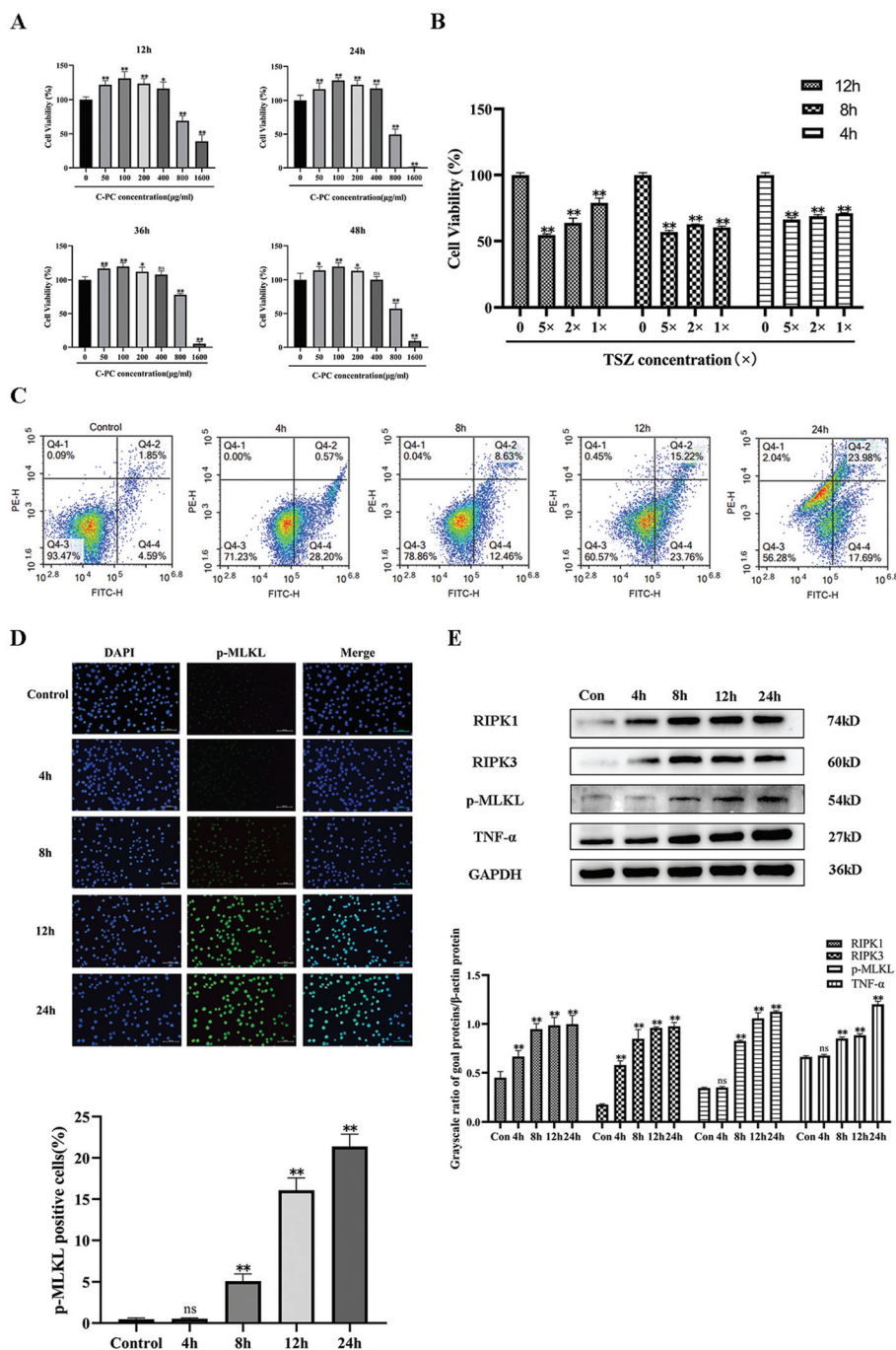


Fig. 2 Effects of C-phycoerythrin and TSZ on the cell viability of GC-1 cells and the expression of RIPK1, RIPK3, p-MLKL, and TNF- α in GC-1 spg cells. (A) Cell viability of GC-1 spg cells is measured by the CCK8 assay. GC-1 spg cells with C-phycoerythrin treatment for 12, 24, 36, and 48 h. Five samples were analyzed in each group, and the results are presented as mean \pm SD. (B) GC-1 spg cells with TSZ treatment for 4, 8, and 12 h. Five samples were analyzed in each group, and the results are presented as mean \pm SD. (C) Analysis of GC-1 spg cell death by flow cytometry using Annexin V-FITC and PI. (D) The fluorescence intensity of p-MLKL was detected by immunofluorescence. Scale bar, 100 μ m. Data are expressed as mean \pm SD. (E) The expression of RIPK1, RIPK3, p-MLKL, and TNF- α were determined by western blot. Data are expressed as mean \pm SD. TSZ, TNF α + Smac mimetic + zVAD-fmk, is a necroptosis inducer. ns, no difference vs. 0 or control group. *, $p < 0.05$ vs. 0 or control group. **, $p < 0.01$ vs. 0 or control group.

treatment group was decreased compared with the control group, while cell viability was increased in the TSZ + C-PC and TSZ + Nec-1 treatment group compared with the TSZ treatment

group (Fig. 3A). Flow cytometry showed that the percentage of necroptotic cells in the TSZ treatment group was 24.01% compared with the control group (0.88%), while the percentage of

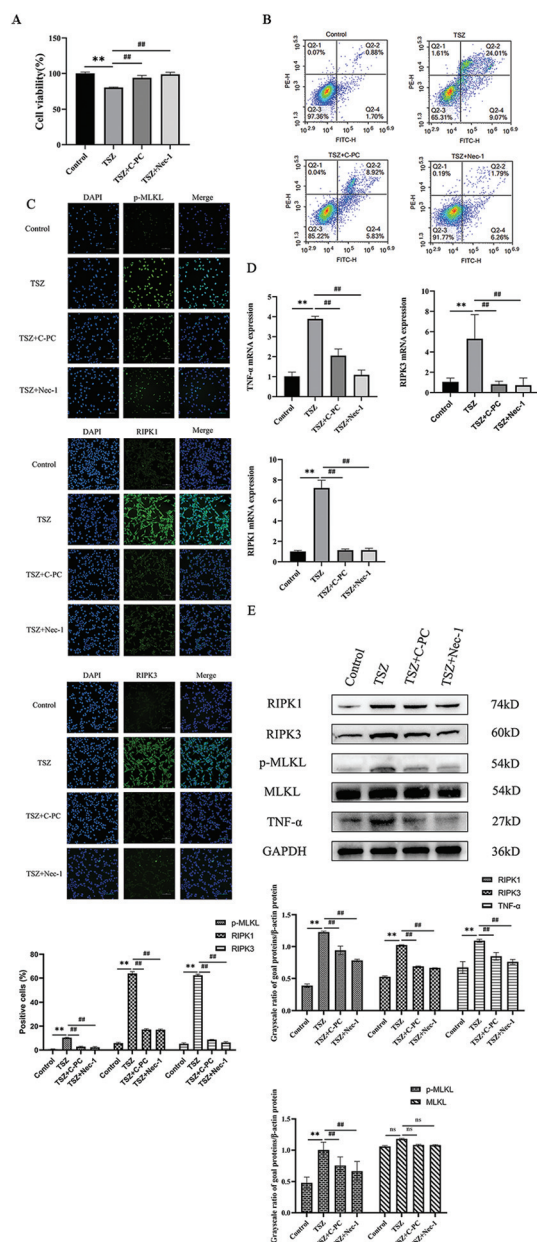


Fig. 3 Effects of C-phycocyanin on cell viability and the expression of RIPK1, RIPK3, p-MLKL, MLKL, and TNF- α in GC-1 spg cells treated with TSZ. (A) Cell viability of GC-1 spg cells is measured by the CCK8 assay. GC-1 spg cells were treated with TSZ for 12 h and treated with C-phycocyanin for 24 h. Five samples were analyzed in each group, and the results are presented as mean \pm SD. (B) Analysis of GC-1 spg cell death by flow cytometry using Annexin V-FITC and PI. GC-1 spg cells were treated with TSZ for 12 h and treated with C-phycocyanin for 24 h. (C) The fluorescence intensity of RIPK1, RIPK3, and p-MLKL was detected by immunofluorescence. Scale bar, 100 μ m. Data are expressed as mean \pm SD. (D) The mRNA level of TNF- α , RIPK1, and RIPK3 in GC-1 spg cells was detected by qRT-PCR. GC-1 spg cells were treated with TSZ for 12 h and treated with C-phycocyanin for 24 h. Data are expressed as mean \pm SD. (E) RIPK1, RIPK3, p-MLKL, MLKL, and TNF- α expression levels in GC-1 spg cells were determined using western blot. GC-1 spg cells were treated with TSZ for 12 h and treated with C-phycocyanin for 24 h. Data are expressed as mean \pm SD. *, $p < 0.05$ vs. control group, **, $p < 0.01$ vs. control group. #, $p < 0.05$ vs. TSZ group. ##, $p < 0.01$ vs. TSZ group.

necroptotic cells was 8.92% in the TSZ + C-PC treatment group and 1.79% in the TSZ + Nec-1 treatment group (Fig. 3B). Then, the expression of three key proteins, RIPK1, RIPK3, and p-MLKL, was detected by immunofluorescence assay. After TSZ treatment, the fluorescence intensity of p-MLKL, RIPK1 and RIPK3 increased compared with the control group. However, they were decreased in TSZ + C-PC and TSZ + Nec-1 treatment groups (Fig. 3C). To investigate the effect of C-PC on the mRNA level of necroptosis-related TNF- α , RIPK1, RIPK3, GC-1 spg cells were treated by TSZ in the presence and absence of C-PC and Nec-1, then evaluated by qRT-PCR. In TSZ-induced GC-1 spg cells, the expression of TNF- α , RIPK1, RIPK3 were markedly increased compared with the control group. However, in the TSZ + C-PC treatment group, they were decreased, the same as in the TSZ + Nec-1 treatment group (Fig. 3D). In addition, we further detected the expression of RIPK1, RIPK3, p-MLKL, MLKL, and TNF- α at the protein level. The results showed that TSZ up-regulated the expression of RIPK1, RIPK3, p-MLKL, and TNF- α , while after the addition of C-PC and Nec-1, they were down-regulated (Fig. 3E). The expression of the protein is consistent with the expression at the mRNA level. In conclusion, these results suggested that C-PC might inhibit necroptosis induced by TSZ by reducing the expression of related transcription factors.

3.4 Organ index of testis and epididymis

Compared with the control group, the organ indexes of testis and epididymis were both significantly decreased in the Cy model group, treated with 50 mg kg⁻¹ Cy for 10 days. However, they were increased in the Cy + C-PC (low) group compared with the Cy model group. Moreover, the effect was even better in Cy + C-PC (high) group. The results suggested that C-PC protects the reproductive organs from damage caused by Cy (Table 1).

3.5 Detection of the quality level of semen

Compared with the control group, Cy-treatment significantly reduced the number of sperms in sperm suspensions of each mouse. However, in Cy + C-PC (low) group, the number of sperm was increased compared to that in the Cy model group, the same as in Cy + C-PC (high) group, and it was even better than low-dose C-PC (Fig. 4A). In addition, Cy-treatment can also lead to sperm malformation. Sperm with head deformity were counted at high magnification using eosin staining. In

Table 1 Effect of C-PC on the organ indexes of testis and epididymis in mice induced by Cy ($\bar{x} \pm S$, mg g⁻¹)

Group	Organ index of testis	Organ index of epididymis
Control	7.86 \pm 0.85	1.77 \pm 0.13
Cy model	5.89 \pm 0.47**	1.21 \pm 0.06**
Cy + C-PC (low)	7.91 \pm 0.72###	1.41 \pm 0.15#
Cy + C-PC (high)	8.27 \pm 0.54###	1.58 \pm 0.23###

The values are expressed as mean \pm SEM. * $P < 0.05$, ** $P < 0.01$ vs. control group. # $P < 0.05$, ### $P < 0.01$ vs. Cy model group.

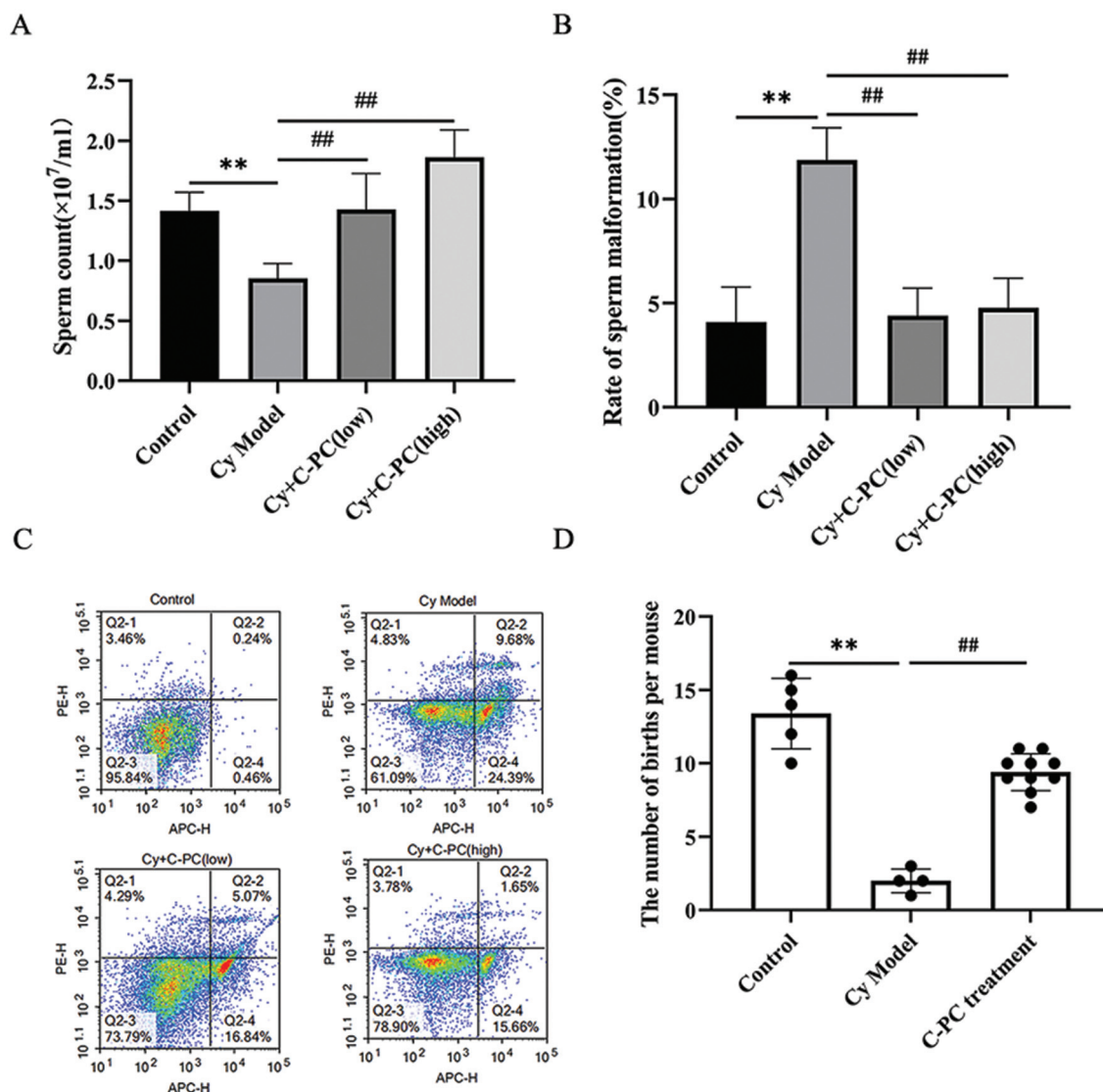


Fig. 4 Effects of C-phycocyanin and cyclophosphamide on the fecundity of mice. (A) The number of sperm in mouse sperm suspension was calculated by cell counting chamber slides. Data are expressed as mean \pm SD. (B) Sperm with head deformities were counted at high magnification using eosin staining. Data are expressed as mean \pm SD. (C) Analysis of sperm death by flow cytometry using Annexin V-FITC and APC. (D) The number of pups per female mouse. Data are expressed as mean \pm SD. *, $p < 0.05$ vs. control group; **, $p < 0.01$ vs. control group. #, $p < 0.05$ vs. Cy model group. ##, $p < 0.01$ vs. Cy model group.

the Cy model group, the mouse of sperm malformation increased significantly compared with the control group, while in the C-PC-treatment group, the mouse of sperm malformation decreased compared with the Cy model group, and with the increase of C-PC concentration, the protective effects were significantly increased (Fig. 4B). The mortality of mice sperm was determined by flow cytometry. The mortality rate of mice sperm in the control group was 0.24%, 9.68% in the Cy model group, 5.07% in Cy + C-PC (low) group, 1.65% in Cy + C-PC (high) group (Fig. 4C). The number of fetal mice was counted, Cy treatment significantly reduced the number of fetal mice. In addition, many female mice that were caged with Cy-treated male mice did not become pregnant, and many fetal mice also died. But in the C-PC group, the number

of fetal mice and pregnant mice were significantly increased (Fig. 4D). These results suggested that C-PC could protect spermatogenic ability and improve the fertility of mice.

3.6 Antioxidant parameters of testis

The contents of MDA in testis tissue of mice in the Cy model group were increased compared with the control group. Compared with the Cy model group, MDA levels were decreased in Cy + C-PC (low) group, and the effect was even better in Cy + C-PC (low) group. Compared with the control group, the activities of SOD were decreased in the Cy model group. However, compared with the Cy model group, the activities of SOD were increased in Cy + C-PC (low) group, the same as in Cy + C-PC (high) group (Table 2). This suggested that

Table 2 Effects of C-PC on antioxidant parameters of testis in mice induced by Cy(\bar{x} + S)

	MDA (nmol per mg prot)	SOD (U ml ⁻¹)
Control	0.20 ± 0.01	1.007 ± 0.05
Cy model	0.44 ± 0.008**	0.116 ± 0.002**
Cy + C-PC (low)	0.25 ± 0.05###	0.632 ± 0.01###
Cy + C-PC (high)	0.19 ± 0.03###	1.07 ± 0.12###

***P* < 0.01 vs. control group. #*P* < 0.05, ###*P* < 0.01 vs. Cy model group.

C-PC could improve antioxidant activity, and high concentrations of C-PC are more protective.

3.7 Serum level of hormones

Serum levels of these three hormones were detected by ELISA kit, including testosterone (T), follicle-stimulating hormone (FSH), luteinizing hormone (LH). The levels of these three hormones were significantly decreased in the Cy model group compared with the control group. But, compared with the Cy model group, the levels of these three hormones were increased in Cy + C-PC (low) group, the same as in Cy + C-PC (high) group, and high concentrations of C-PC were more effective (Table 3).

3.8 The histopathological evaluation of the testes and kidneys

Since Cy can cause histopathological changes, HE staining was used to observe the morphological changes of the testes of the mice after Cy and C-PC treatment. The morphology of the kidneys was also examined considering their relationship to reproduction.

In the control group, the basal membrane of the seminiferous tubules was intact, the seminiferous epithelium was thicker, the seminiferous cells were numerous, orderly and normal in shape, and a large number of spermatids and sperm could be seen in the lumen. But in the model group, the epithelial cells of the seminiferous tubules were thinned, the number of seminiferous cells was reduced, and the empty cavity was formed in the lumen. In the C-PC-treatment group, the seminiferous tubule damage improved to varying degrees, and the spermatogenic cells increased, while the arrangement was neat and orderly, with a marked decrease in the cavity. A high concentration of C-PC was more effective than a low concentration (Fig. 5A). A cross-section of the kidneys showed

Table 3 Effects of C-PC on the serum level of hormones in mice induced by Cy(\bar{x} + S)

Group	T (ng ml ⁻¹)	FSH (mIU ml ⁻¹)	LH (mIU ml ⁻¹)
Control	16.27 ± 0.58	65.78 ± 1.73	11.07 ± 0.54
Cy model	9.49 ± 0.45**	38.94 ± 0.94**	7.03 ± 0.33**
Cy + C-PC (low)	16.29 ± 0.64###	69.08 ± 1.68###	8.39 ± 0.14#
Cy + C-PC (high)	16.75 ± 0.70###	69.47 ± 3.71###	9.16 ± 0.93###

***P* < 0.01 vs. control group. #*P* < 0.05, ###*P* < 0.01 vs. Cy model group.

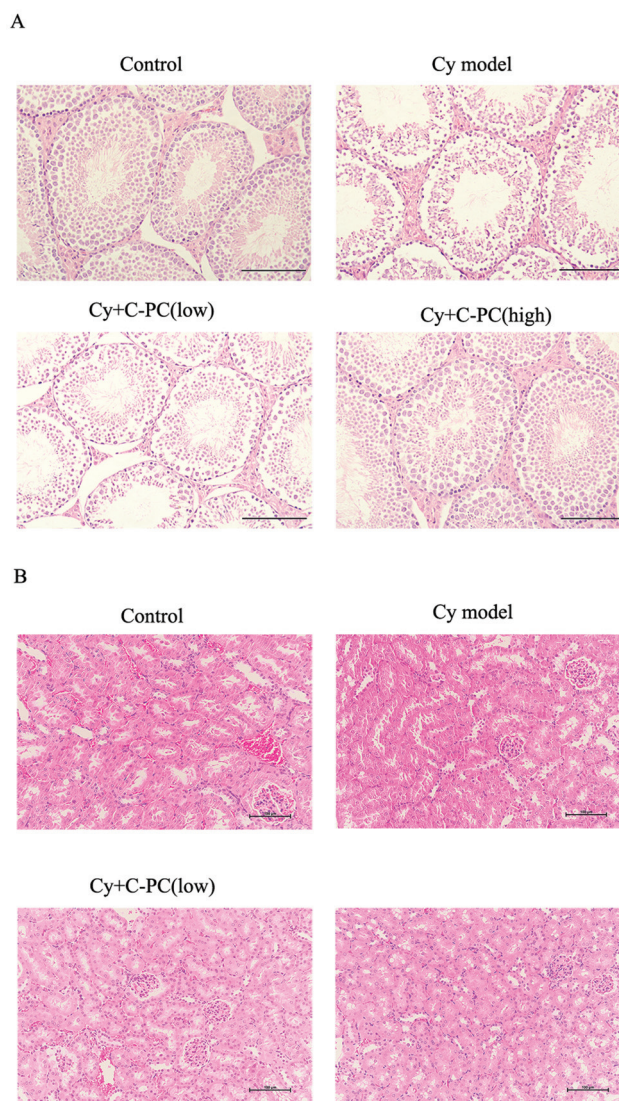


Fig. 5 (A) Microscopic photos of HE histological staining of mice testes. Scale bar 50 μm. (B) Microscopic photos of HE histological staining of mice kidneys. Scale bar 100 μm.

clearly defined renal capsules in the mice of the control group, while the shape of the blood vessels was normal, the basement membrane was intact, and the shape of the renal tubules was typical. In the Cy model group, the renal corpus was swollen and deformed, while both the renal capsule space and intratubular space became smaller, and the border was blurred. The swollen and deformed kidneys of the mice in C-PC (low) and C-PC (high) were improved to some extent but still differed from the control group (Fig. 5B).

3.9 Histopathological analysis of testis

In order to analyze the spermatogenic dynamics of mice, we stained the testicular tissue sections with HE, and then evaluated the cell populations of the seminiferous tubule sections and counted them. As shown in Fig. 6A, in the control group, all kinds of cells in seminiferous tubules were distinct and

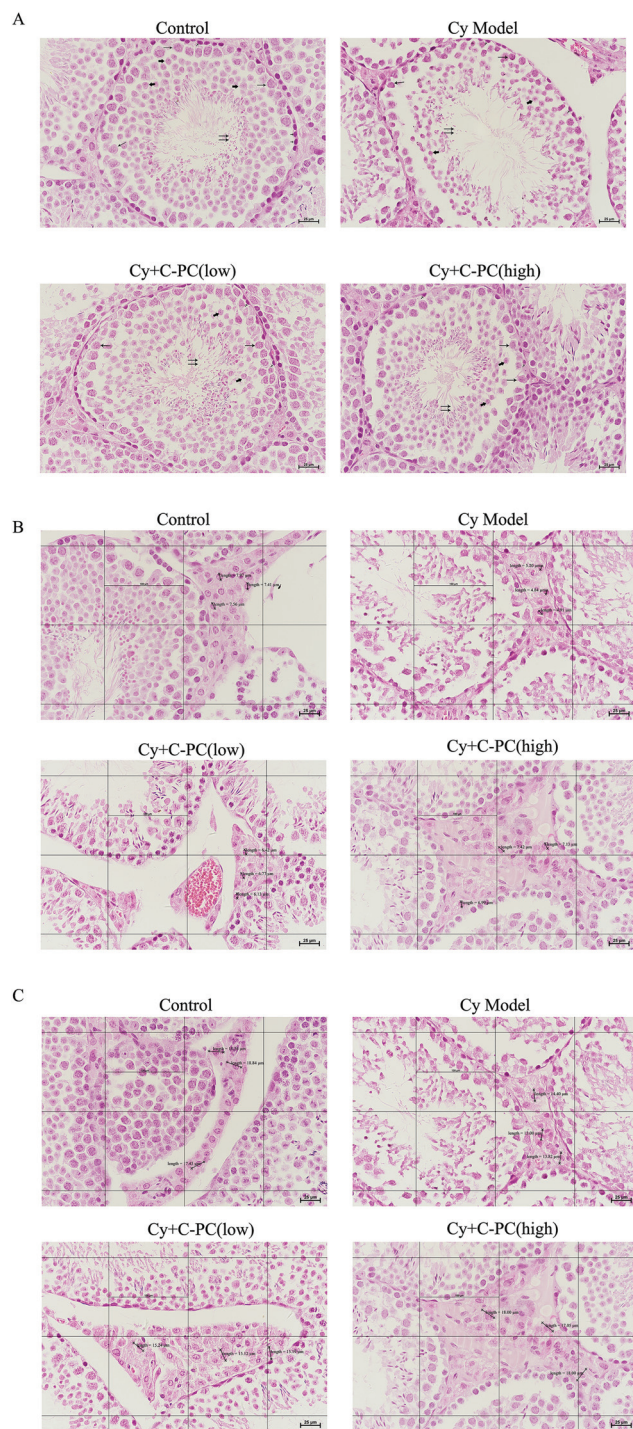


Fig. 6 Histopathological analysis of testis in mice. (A) The cell population of the seminiferous tubule. Spermatogonium (short arrow), primary spermatocytes (long arrow), secondary spermatocytes (coarse arrow), spermatid (double-headed arrow). (B) Nuclear diameter of Leydig cells. (C) The diameter of Leydig cells. Scale bar 25 μm .

neatly arranged. The spermatogonium (short arrow) was close to the spermatogenic epithelial basement membrane, and the cells were round or oval in shape. The primary spermatocytes (long arrow) were located near the cavity side of the spermatogonium,

which was round and large in volume. Secondary spermatocytes (coarse arrow) were located on the distal cavity side of the spermatogonia, and the volume was half that of primary spermatocytes. The spermatids (double-headed arrows) were located in the center of the lumen and were shaped like a tadpole. In the Cy model group, the arrangement of all kinds of cells was chaotic, the number of cells visible to the naked eye decreased, and the empty cavity was formed in the lumen. In the C-PC treatment group, all kinds of cells in the seminiferous tubules were arranged neatly, and a large number of spermatids could be seen in the center of the lumen. Then, we counted all kinds of cells in each seminiferous tubule under a light microscope and found that compared with the control group (Table 4), the number of spermatogonium, primary spermatocytes, secondary spermatocytes and spermatids in the Cy model group decreased significantly, while in C-PC (low) group, compared with the Cy model group, the number of all kinds of cells increased, and the effect of C-PC (high) group was better.

As shown in Fig. 6B and C, we measured the diameter of Leydig cells and nucleus. Through statistical study, it was found that the diameter and volume of Leydig cells and nucleus decreased, compared with the control group. While in C-PC (low) group, compared with the Cy model group, the diameter and volume of Leydig cells and nucleus were increased, and high concentrations of C-PC were more effective (Table 5).

3.10 C-phycoerythrin protects the reproductive system from cyclophosphamide damage by inhibiting the necroptotic signaling pathway

The expression of p-MLKL, RIPK1, RIPK3 in testicular tissue were detected by immunohistochemistry. In the Cy model group, the expression of p-MLKL, RIPK1, RIPK3 were increased compared with the control group. However, in the C-PC treated group, they were decreased compared with the Cy model group, and a high concentration of C-PC was more effective than a low concentration (Fig. 7A). In addition, the results were further approved by western blot. These results are consistent with immunohistochemical results (Fig. 7B). These results suggested that Cy treatment induced inflammatory damage in the reproductive system and activated the TNF- α signaling pathway, leading to up-regulation of RIPK1, RIPK3, and MLKL. After pre-treatment with C-PC, the expression of RIPK1, RIPK3, and MLKL was down-regulated, so the necroptosis signaling pathway was prevented, thus C-PC played a certain protective role in the reproductive system.

4. Discussion

In the second decade of the new millennium, infertility remains a very common condition globally.⁴¹ Infertility is estimated to affect 9% of reproductive-aged couples currently cited as the probable global average.⁴² However, in some parts of the world, the rates of infertility are as high as 30% in some populations.⁴³ This is particularly true in regions with high

Table 4 The number of germ cells in seminiferous tubules of testicular tissue of mice ($\bar{x} \pm S$)

Group	Spermatogonium	Primary spermatocytes	Secondary spermatocytes	Spermatid
Control	62.83 ± 2.86	56.33 ± 3.44	125.3 ± 8.04	168.2 ± 8.93
Cy model	35.17 ± 2.22**	31.67 ± 2.50**	78.67 ± 11.84**	110.3 ± 15.15**
Cy + C-PC (low)	53.17 ± 1.94 ^{###}	44.5 ± 2.59 ^{###}	114.7 ± 11.33 ^{###}	149.3 ± 10.37 ^{###}
Cy + C-PC (high)	60.00 ± 2.0 ^{###}	52.00 ± 4.15 ^{###}	119.3 ± 10.86 ^{###}	157.3 ± 10.17 ^{###}

** $P < 0.01$ vs. control group. ^{###} $P < 0.01$ vs. Cy model group.

Table 5 Diameter and volume of Leydig cells and nuclear in testis ($\bar{x} \pm S$)

Group	Nuclear diameter of Leydig cells (μm)	Nuclear volume of Leydig cells (μm^3)	The diameter of Leydig cells (μm)	The volume of Leydig cells (μm^3)
Control	7.551 ± 0.28	226.2 ± 25.12	17.91 ± 0.60	3017 ± 306.5
Cy model	5.501 ± 0.40**	88.36 ± 18.46**	13.54 ± 0.73**	1308 ± 208.3**
Cy + C-PC (low)	6.341 ± 0.26 ^{###}	134.2 ± 17.39 ^{###}	15.44 ± 0.38 ^{###}	1929 ± 143.7 ^{###}
Cy + C-PC (high)	7.151 ± 0.26 ^{###}	192.1 ± 21.45 ^{###}	17.62 ± 0.50 ^{###}	2867 ± 242.3 ^{###}

** $P < 0.01$ vs. control group. ^{###} $P < 0.01$ vs. Cy model group.

rates of infertility, including South Asia, sub-Saharan Africa, the Middle East and North Africa, Central and Eastern Europe and other countries.⁴⁴ As a result, in most developing countries, infertile men were commonly prescribed botanical medicines that improved sperm quality, sexual functions, libido and testosterone levels.⁴⁵ Medicinal plants that are used to treat infertility have been empirically used as extracts, decoctions, or partially purified compounds. These herbal remedies are used to treat impaired libido, sexual weakness, erectile dysfunction, ejaculatory disorders and defective sperm production (azoospermia, oligospermia).⁴⁶ Although many medicinal plants could be used to improve sexual dysfunction, most of the drugs have strong side effects and could cause the failure of other organs, such as the heart, liver and lungs. Most of these drugs have yet to pass clinical tests for formal clinical use.⁴⁷ Their mechanism of action in the body is also unknown, so people have turned to the ocean. As a treasure house of natural medicines, the ocean has many resources that can be exploited and utilized.⁴⁸

C-phycoerythrin is a biologically active nutrient compound that is isolated and purified from a variety of *Spirulina platensis*.⁴⁹ In recent years, many studies have demonstrated that C-phycoerythrin is useful for animal health, and especially to reproductive function.^{23–25} However, there are few reports of the effects of C-phycoerythrin on the male reproductive system.

GC-1 spg cells as experimental subjects and sought to induce necroptosis in these cell lines to construct a cellular model necroptosis. TSZ, TNF α + Smac mimetic + zVAD-fmk, is a necroptosis inducer. HT29 that could be induced by TSZ is the earliest and most commonly used cell model for studying necroptosis. Wang *et al.* used this model in a series of studies and revealed the classic necroptotic RIPK1/RIPK3/MLKL pathway.^{34,50,51} In addition, they injected TSZ into the testes of 2-month-old mice and found that injection of TSZ directly into the testis induced MLKL phosphorylation. *In vitro* experiments

have also confirmed that TSZ-induced cells in the seminiferous tubules, including spermatogonia, Sertoli cells, and spermatocytes, were stained positive for p-MLKL.³⁷ In our study, the proliferation activity of TSZ-induced GC-1 spg cells decreased significantly. We designed five treated periods, including 0 h, 4 h, 8 h, 12 h, and 24 h, respectively, and found that cell viability gradually decreased with the extension of time. Flow cytometry also showed that the number of necrotic cells gradually increased with time, which indicated that TSZ could lead to the death of GC-1 cells. In order to further explore the mode of cell death, we detected the expression of p-MLKL in cells, which is a currently well-recognized marker of necroptosis.⁵² The number of p-MLKL positive cells increased gradually with the increase of time. We also verified the expression of necroptosis-related proteins in TSZ-induced GC-1 spg cells. Similarly, the expression of these proteins increased gradually in a time-dependent manner. These results suggested that the GC-1 spg cell lines could be used as a model for TSZ-induced necroptosis.

After the successful establishment of the necroptosis model with GC-1 spg cells, we investigated the specific role of C-phycoerythrin in the RIPK1/RIPK3/MLKL signaling pathway. Before TSZ-induced cells, we pretreated the cells with C-phycoerythrin for 12 h, and we used Necrostatin-1 (Nec-1) as a positive control. Necrostatin-1, is a TNF- α inhibitor, can rescue cell death.⁵³ We found that cell viability decreased after TSZ induction, while in the C-phycoerythrin treated group, cell viability increased significantly and death cells decreased, suggesting that C-phycoerythrin can protect cells from TSZ damage.

Necroptosis is a form of regulated cell death, which is induced by ligand binding to TNF family death domain receptors, pattern recognizing receptors and virus sensors, RIPK1, RIPK3 and p-MLKL is the key protein to necroptotic pathway.⁵⁴ In cells, necroptosis can be initiated by a variety of triggers,

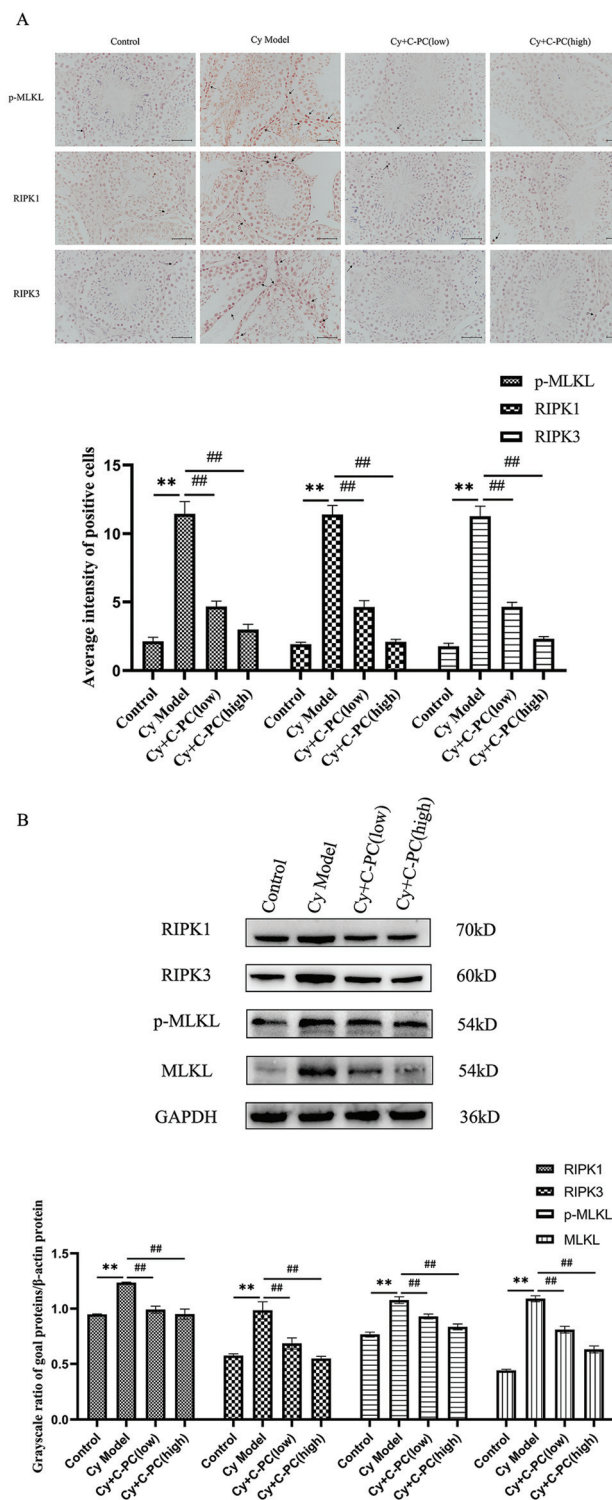


Fig. 7 The expression of p-MLKL, RIPK1, RIPK3, and MLKL in testicular tissue. (A) The expression of p-MLKL, RIPK1, and RIPK3 in testicular tissue by immunohistochemistry. Scale bar 50 μ m. (B) The expression of p-MLKL, RIPK1, RIPK3, and MLKL in testicular tissue by western blot. Data are expressed as mean \pm SD. * p < 0.05, ** p < 0.01 vs. Control group. # p < 0.05, ## p < 0.01 vs. Cy model group.

including TNF, Fas, TNF-related apoptosis-inducing ligand (TRAIL), interferon (IFN).^{55–57} The expressions of RIPK1, RIPK3, p-MLKL and other proteins were up-regulated in the cells treated with TSZ, while the expressions of these proteins were down-regulated in the C-PC-pretreated group. The trend of these genes at the mRNA level is the same as proteins.

In addition, to verify at the cellular level, we also conducted animal experiments. Cyclophosphamide was used to construct the reproductive injury model. Cyclophosphamide is a widely used chemotherapy drug in clinical practice, but its toxic side effects are strong, such as cytotoxicity and infertility.⁵⁸ It can damage the production and quality of sperm, thus leading to an increased incidence of azoospermia and oligozoospermia.⁵⁹ Cyclophosphamide disrupts cell growth and differentiation and can lead to increased DNA damage, oxidative stress and protamine retention. Its male reproductive toxicity is usually characterized by oligozoospermia, azoospermia, changes in testicular tissue toxic testosterone levels, and oxidative emergency parameters.^{60–64} High-dose injection of cyclophosphamide can cause damage to reproductive organs. The testicular and epididymal coefficients of the cyclophosphamide-treated mice were reduced, while those of the C-PC – treated mice were similar to those of the normal control group. This suggested that the injection of cyclophosphamide in high-dose, caused atrophy of reproductive organs, and C-phycoerythrin could play a certain protective role on reproductive organs, preventing them from being damaged by cyclophosphamide. The histopathological evaluation of the testes also confirmed this conclusion. The testicular tissue of mice treated with cyclophosphamide was significantly damaged. The epithelial cells of the seminiferous tubules were thinned, the number of seminiferous cells were reduced, and the cavity was formed in the lumen. In the C-PC-treated group, this damage was significantly reduced due to the protective effect of C-phycoerythrin. We also evaluated the cell populations of the seminiferous tubule sections. In the Cy model group, the number of spermatogonium, primary spermatocytes, secondary spermatocytes and spermatids decreased significantly, while in the C-PC treatment group, the number of these germ cells increased. These results have shown that C-PC could protect mouse testicular tissue from Cy damage and ensure the spermatogenic ability of mice.

Hypogonadism in men is a clinical syndrome characterized by low testosterone and/or low sperm count.⁶⁵ Hypogonadism can be roughly divided into primary, secondary and mixed hypogonadism based on defects in the testis, hypothalamus and/or pituitary gland. The measurement of serum testosterone is often the single most important diagnostic test for male hypogonadism.^{65,66} Patients with primary hypogonadism have low testosterone levels and elevated luteinizing hormone (LH) and follicle-stimulating hormone (FSH). Patients with secondary hypogonadism have low testosterone levels, low or inappropriately normal LH and FSH.^{67,68} In our study, to test the gonadal function of mice, the serum levels of testosterone, FSH and LH were measured. It was found that the levels of testosterone, FSH and LH decreased in cyclophosphamide treated

mice, indicating that cyclophosphamide caused gonadal dysfunction in mice, resulting in an imbalance of sex hormone levels and affecting the spermatogenic ability of mice. However, the levels of these three hormones in the C-phycoyanin-treated mice were all at normal levels. In addition, we also measured the volume of Leydig cells and nuclei. In the Cy model group, the volume of Leydig cells and nucleus decreased, indicating that Cy caused a certain degree of damage to Leydig cells and made their function abnormal. In the C-PC treatment group, the degree of injury of Leydig cells was significantly reduced, and the function was relatively normal. These results indicated that C-PC-treated mice had a certain protective effect on their gonads, which could protect them from Cy damage and ensure the normal hormone regulation level and sperm-producing ability of mice.

The quality of male sperm is an important basis to evaluate the health of the male reproductive system, which directly affects the ability and quality of reproduction.^{69,70} In our study, cyclophosphamide produced great damage to the quality of sperm in male mice, resulting in a decrease in concentration and number of sperm, and a significant increase in sperm malformation, resulting in the decline of spermatogenic ability of male mice, severely damaged reproductive function. The C-PC-pretreated mice showed significant improvements in sperm quantities and concentration, reduced rates of sperm malformation, and improved fertility. C-phycoyanin could protect the reproductive system of mice to some extent and ensure the sperm quality and fertility of mice.

In order to determine whether the protective effect of C-phycoyanin on the reproductive system is related to the necroptotic signaling pathway, we detected the key proteins in the pathway, respectively. We found that the expressions of RIPK1, RIPK3, MLKL, and p-MLKL were upregulated after cyclophosphamide treatment, suggesting that cyclophosphamide stimulated the necroptotic signaling pathway and upregulated the expressions of key molecules. However, C-phycoyanin treatment can down-regulate the expressions of RIPK1, RIPK3, MLKL and p-MLKL, indicating that C-phycoyanin can prevent cyclophosphamide from activating the necroptotic signaling pathway and protect the reproductive system through this effect.

5. Conclusion

This study demonstrated that C-phycoyanin could prevent GC-1 spg cells from damage by TSZ-induced necroptosis, improve cell viability and down-regulate the necroptotic signaling pathway, thus playing a certain protective role on GC-1 spg cells. Moreover, C-phycoyanin could protect the reproductive system of mice by improving the cyclophosphamide-induced decrease of the concentration of sperm and reducing the rate of occurrence of deformities in sperm. The protection mechanism might be such that C-phycoyanin could inhibit the oxidative stress and necroptosis of reproductive-related cells induced by cyclophosphamide and C-phycoyanin could play

its protective role by inhabiting the necroptotic signaling pathway. These results suggested that C-phycoyanin could serve as a promising reproductive system protective agent during the development of the reproductive system.

Author contributions

Fanghao Yang: Writing – original draft, data curation, resources; Xiaolei Dong: formal analysis, data curation; Guoxiang Liu: validation, formal analysis; Lei Teng: project administration; Lin Wang: resources, investigation; Feng Zhu: methodology; Fenghua Xu: supervision; Yifan Yang: software; Can Cao: investigation; Guang Chen: methodology; Bing Li: conceptualization, writing – review & editing.

Ethical statement

All animal procedures were performed in accordance with the Guidelines for Care and Use of Laboratory Animals of “Qingdao” University and experiments were approved by the Animal Ethics Committee of “Ethics Committee Medical College of Qingdao University”.

Conflicts of interest

The authors have declared that no competing interest exists.

Acknowledgements

This work was supported by grants from the National Natural Science Foundation of China (No. 81871231, 81471546 and 81001346), Youth Innovation and Technology Plan of Shandong Province (2019KJK016), and Qingdao Civic Science and Technology Project (No. 18-6-1-91-nsh).

References

- 1 A. Agarwal, S. Baskaran, N. Parekh, C.-L. Cho, R. Henkel, S. Vij, M. Arafa, M. K. Panner and S. R. Shah, Male infertility, *Lancet*, 2021, **397**, 319–333.
- 2 M. G. Barbu, D. C. Thompson, N. Suci, S. C. Voinea, D. Cretoiu and D. V. Predescu, The Roles of MicroRNAs in Male Infertility, *Int. J. Mol. Sci.*, 2021, **22**, 2910.
- 3 A. Agarwal, A. Mulgund, A. Hamada and M. R. Chyatte, A unique view on male infertility around the globe, *Reprod. Biol. Endocrinol.*, 2015, **13**, 37.
- 4 A. Ilacqua, G. Izzo, G. P. Emerenziani, C. Baldari and A. Aversa, Lifestyle and fertility: the influence of stress and quality of life on male fertility, *Reprod. Biol. Endocrinol.*, 2018, **16**, 115.
- 5 C. Krausz and A. Riera-Escamilla, Genetics of male infertility, *Nat. Rev. Urol.*, 2018, **15**, 369–384.

- 6 C. H. Glazer, M. L. Eisenberg, S. S. Tøttenborg, A. Giwercman, E. M. Flachs, E. V. Bräuner, D. Vassard, A. Pinborg, L. Schmidt and J. P. Bonde, Male factor infertility and risk of death: a nationwide record-linkage study, *Hum. Reprod.*, 2019, **34**, 2266–2273.
- 7 C. Krausz, Male infertility: pathogenesis and clinical diagnosis, *Best Pract. Res., Clin. Endocrinol. Metab.*, 2011, **25**, 271–285.
- 8 A. Salonia, C. Bettocchi, L. Boeri, P. Capogrosso, J. Carvalho, N. C. Cilesiz, A. Cocci, G. Corona, K. Dimitropoulos, M. Gül, *et al.*, European Association of Urology Guidelines on Sexual and Reproductive Health-2021 Update: Male Sexual Dysfunction, *Eur. Urol.*, 2021, **80**, 333–357.
- 9 A. Agarwal, N. Parekh, M. K. Panner Selvam, R. Henkel, R. Shah, S. T. Homa, R. Ramasamy, E. Ko, K. Tremellen, S. Esteves, *et al.*, Male Oxidative Stress Infertility (MOSI): Proposed Terminology and Clinical Practice Guidelines for Management of Idiopathic Male Infertility, *World J. Mens Health*, 2019, **37**, 296–312.
- 10 Y. Ma, X. He, K. Qi, T. Wang, Y. Qi, L. Cui, F. Wang and M. Song, Effects of environmental contaminants on fertility and reproductive health, *J. Environ. Sci.*, 2019, **77**, 210–217.
- 11 S. Ghafouri-Fard, H. Shoorei, A. Abak, M. Seify, M. Mohaqiq, F. Keshmir, M. Taheri and S. A. Ayatollahi, Effects of chemotherapeutic agents on male germ cells and possible ameliorating impact of antioxidants, *Biomed. Pharmacother.*, 2021, **142**, 112040.
- 12 A. G. Hall and M. J. Tilby, Mechanisms of action of, and modes of resistance to, alkylating agents used in the treatment of haematological malignancies, *Blood Rev.*, 1992, **6**, 163–173.
- 13 S. Al-Aqbi, N. M. Al-Sharafi and H. Al-Salih, The Pathological Features of Cyclophosphamide Induced Multi-Organ Toxicity in Male Wister Rats, *Syst. Rev. Pharm.*, 2020, **11**, 45–49.
- 14 A. R. Iraqi and N. Adnan, Effect of Cyclophosphamide Treatment During the Embryonic Period on Fertility of Adult Male Mice, *Iraqi J. Sci.*, 2019, **60**, 706–714.
- 15 G. Nayak, A. Rao, P. Mullick, S. Mutalik, S. G. Kalthur, S. K. Adiga and G. Kalthur, Ethanolic extract of *Moringa oleifera* leaves alleviate cyclophosphamide-induced testicular toxicity by improving endocrine function and modulating cell specific gene expression in mouse testis, *J. Ethnopharmacol.*, 2020, **259**, 112922.
- 16 S. Benedetti, S. Rinalducci, F. Benvenuti, S. Francogli, S. Pagliarani, L. Giorgi, M. Micheloni, G. M. D'Amici, L. Zolla and F. Canestrari, Purification and characterization of phycocyanin from the blue-green alga *Aphanizomenon flos-aquae*, *J. Chromatogr. B: Anal. Technol. Biomed. Life Sci.*, 2006, **833**, 12–18.
- 17 R. P. Rastogi, R. R. Sonani and D. Madamwar, Effects of PAR and UV Radiation on the Structural and Functional Integrity of Phycocyanin, Phycocerythrin and Allophycocyanin Isolated from the Marine Cyanobacterium *Lyngbya* sp. A09DM, *Photochem. Photobiol.*, 2015, **91**, 837–844.
- 18 I. N. Stadnichuk, P. M. Krasil'nikov and D. V. Zlenko, [Cyanobacterial Phycobilisomes and Phycobiliproteins], *Mikrobiologiya*, 2015, **84**, 131–143.
- 19 Q. Wu, L. Liu, A. Miron, B. Klímová, D. Wan and K. Kuča, The antioxidant, immunomodulatory, and anti-inflammatory activities of *Spirulina*: an overview, *Arch. Toxicol.*, 2016, **90**, 1817–1840.
- 20 K. R. Roy, K. M. Arunasree, N. P. Reddy, B. Dheeraj, G. V. Reddy and P. Reddanna, Alteration of mitochondrial membrane potential by *Spirulina platensis* C-phycocyanin induces apoptosis in the doxorubicin-resistant human hepatocellular-carcinoma cell line HepG2, *Biotechnol. Appl. Biochem.*, 2007, **47**, 159–167.
- 21 C. Romay, R. González, N. Ledón, D. Ramirez and V. Rimbau, C-phycocyanin: a biliprotein with antioxidant, anti-inflammatory and neuroprotective effects, *Curr. Protein Pept. Sci.*, 2003, **4**, 207–216.
- 22 B. Li, X. M. Chu, Y. J. Xu, F. Yang, C. Y. Lv and S. M. Nie, CD59 underlines the antiatherosclerotic effects of C-phycocyanin on mice, *BioMed Res. Int.*, 2013, **2013**, 729413.
- 23 X. Wen, Z. Han, S. J. Liu, X. Hao, X. J. Zhang, X. Y. Wang, C. J. Zhou, Y. Z. Ma and C. G. Liang, Phycocyanin Improves Reproductive Ability in Obese Female Mice by Restoring Ovary and Oocyte Quality, *Front. Cell Dev. Biol.*, 2020, **8**, 595373.
- 24 Y. J. Niu, W. Zhou, J. Guo, Z. W. Nie, K. T. Shin, N. H. Kim, W. F. Lv and X. S. Cui, C-Phycocyanin protects against mitochondrial dysfunction and oxidative stress in parthenogenetic porcine embryos, *Sci. Rep.*, 2017, **7**, 16992.
- 25 S. Liang, J. Guo, Y. X. Jin, B. Yuan, J. B. Zhang and N. H. Kim, C-Phycocyanin supplementation during in vitro maturation enhances pre-implantation developmental competence of parthenogenetic and cloned embryos in pigs, *Theriogenology*, 2018, **106**, 69–78.
- 26 A. Linkermann and D. R. Green, Necroptosis, *N. Engl. J. Med.*, 2014, **370**, 455–465.
- 27 Y. K. Dhuriya and D. Sharma, Necroptosis: a regulated inflammatory mode of cell death, *J. Neuroinflammation*, 2018, **15**, 199.
- 28 A. Degtarev, J. Hitomi, M. Germscheid, I. L. Ch'en, O. Korkina, X. Teng, D. Abbott, G. D. Cuny, C. Yuan, G. Wagner, *et al.*, Identification of RIP1 kinase as a specific cellular target of necrostatins, *Nat. Chem. Biol.*, 2008, **4**, 313–321.
- 29 C. C. Smith, S. M. Davidson, S. Y. Lim, J. C. Simpkin, J. S. Hothersall and D. M. Yellon, Necrostatin: a potentially novel cardioprotective agent?, *Cardiovasc. Drugs Ther.*, 2007, **21**, 227–233.
- 30 J. Lin, H. Li, M. Yang, J. Ren, Z. Huang, F. Han, J. Huang, J. Ma, D. Zhang, Z. Zhang, *et al.*, A role of RIP3-mediated macrophage necrosis in atherosclerosis development, *Cell Rep.*, 2013, **3**, 200–210.
- 31 A. Linkermann, J. H. Bräsen, N. Himmerkus, S. Liu, T. B. Huber, U. Kunzendorf and S. Krautwald, Rip1 (receptor-interacting protein kinase 1) mediates necroptosis and

- contributes to renal ischemia/reperfusion injury, *Kidney Int.*, 2012, **81**, 751–761.
- 32 M. I. Oerlemans, J. Liu, F. Arslan, K. den Ouden, B. J. van Middelaar, P. A. Doevendans and J. P. Sluijter, Inhibition of RIP1-dependent necrosis prevents adverse cardiac remodeling after myocardial ischemia-reperfusion in vivo, *Basic Res. Cardiol.*, 2012, **107**, 270.
- 33 J. Wu, Z. Huang, J. Ren, Z. Zhang, P. He, Y. Li, J. Ma, W. Chen, Y. Zhang, X. Zhou, *et al.*, Mkl1 knockout mice demonstrate the indispensable role of Mkl1 in necroptosis, *Cell Res.*, 2013, **23**, 994–1006.
- 34 S. He, L. Wang, L. Miao, T. Wang, F. Du, L. Zhao and X. Wang, Receptor interacting protein kinase-3 determines cellular necrotic response to TNF- α , *Cell*, 2009, **137**, 1100–1111.
- 35 C. Günther, E. Martini, N. Wittkopf, K. Amann, B. Weigmann, H. Neumann, M. J. Waldner, S. M. Hedrick, S. Tenzer, M. F. Neurath, *et al.*, Caspase-8 regulates TNF- α -induced epithelial necroptosis and terminal ileitis, *Nature*, 2011, **477**, 335–339.
- 36 P. S. Welz, A. Wullaert, K. Vlantis, V. Kondylis, V. Fernández-Majada, M. Ermolaeva, P. Kirsch, A. Sterner-Kock and G. van L. M. Pasparakis, FADD prevents RIP3-mediated epithelial cell necrosis and chronic intestinal inflammation, *Nature*, 2011, **477**, 330–334.
- 37 D. Li, L. Meng, T. Xu, Y. Su, X. Liu, Z. Zhang and X. Wang, RIPK1-RIPK3-MLKL-dependent necrosis promotes the aging of mouse male reproductive system, *eLife*, 2017, **6**, e27692.
- 38 Y. Xie, H. Chen, D. Luo, X. Yang, J. Yao, C. Zhang, L. Lv, Z. Guo, C. Deng, Y. Li, *et al.*, Inhibiting necroptosis of spermatogonial stem cell as a novel strategy for male fertility preservation, *Stem Cells Dev.*, 2020, 475–487.
- 39 Y. Xie, L. Lv, J. Yao, C. Zhang, H. Chen, W. Chen, X. Liang, X. Sun, C. Deng and G. Liu, Phosphorylated mixed lineage kinase domain-like protein in human seminal plasma: A potential novel biomarker of spermatogenic function, *Andrologia*, 2019, **51**, e13310.
- 40 S. Pietkiewicz, J. H. Schmidt and I. N. Lavrik, Quantification of apoptosis and necroptosis at the single cell level by a combination of Imaging Flow Cytometry with classical Annexin V/propidium iodide staining, *J. Immunol. Methods*, 2015, **423**, 99–103.
- 41 W. Ombelet, I. Cooke, S. Dyer, G. Serour and P. Devroey, Infertility and the provision of infertility medical services in developing countries, *Hum. Reprod. Update*, 2008, **14**, 605–621.
- 42 J. Boivin, L. Bunting, J. A. Collins and K. G. Nygren, International estimates of infertility prevalence and treatment-seeking: potential need and demand for infertility medical care, *Hum. Reprod.*, 2007, **22**, 1506–1512.
- 43 R. D. Nachtigall, International disparities in access to infertility services, *Fertil. Steril.*, 2006, **85**, 871–875.
- 44 M. N. Mascarenhas, S. R. Flaxman, T. Boerma, S. Vanderpoel and G. A. Stevens, National, regional, and global trends in infertility prevalence since 1990: a systematic analysis of 277 health surveys, *PLoS Med.*, 2012, **9**, e1001356.
- 45 M. Kolahdooz, S. Nasri, S. Z. Modarres, S. Kianbakht and H. F. Huseini, Effects of Nigella sativa L. seed oil on abnormal semen quality in infertile men: a randomized, double-blind, placebo-controlled clinical trial, *Phytomedicine*, 2014, **21**, 901–905.
- 46 S. O. Abarikwu, C. L. Onuah and S. K. Singh, Plants in the management of male infertility, *Andrologia*, 2020, **52**, e13509.
- 47 A. J. Bella and R. Shamloul, Traditional plant aphrodisiacs and male sexual dysfunction, *Phytother. Res.*, 2014, **28**, 831–835.
- 48 P. M. Murray, S. Moane, C. Collins, T. Beletskaya, O. P. Thomas, A. W. Duarte, F. S. Nobre, I. O. Owoyemi, F. C. Pagnocca, L. D. Sette, *et al.*, Sustainable production of biologically active molecules of marine based origin, *NanoBiotechnology*, 2013, **30**, 839–850.
- 49 M. F. de Jesus Raposo, R. M. de Moraes and A. M. de Moraes, Health applications of bioactive compounds from marine microalgae, *Life Sci.*, 2013, **93**, 479–486.
- 50 H. Wang, L. Sun, L. Su, J. Rizo, L. Liu, L. F. Wang, F. S. Wang and X. Wang, Mixed lineage kinase domain-like protein MLKL causes necrotic membrane disruption upon phosphorylation by RIP3, *Mol. Cell*, 2014, **54**, 133–146.
- 51 L. Sun, H. Wang, Z. Wang, S. He, S. Chen, D. Liao, L. Wang, J. Yan, W. Liu, X. Lei, *et al.*, Mixed lineage kinase domain-like protein mediates necrosis signaling downstream of RIP3 kinase, *Cell*, 2012, **148**, 213–227.
- 52 M. Pasparakis and P. Vandenabeele, Necroptosis and its role in inflammation, *Nature*, 2015, **517**, 311–320.
- 53 D. F. Eytan, G. E. Snow, S. Carlson, A. Derakhshan, A. Saleh, S. Schiltz, H. Cheng, S. Mohan, S. Cornelius, J. Coupar, *et al.*, SMAC Mimetic Birinapant plus Radiation Eradicates Human Head and Neck Cancers with Genomic Amplifications of Cell Death Genes FADD and BIRC2, *Cancer Res.*, 2016, **76**, 5442–5454.
- 54 S. Grootjans, T. Vanden and B. P. Vandenabeele, Initiation and execution mechanisms of necroptosis: an overview, *Cell Death Differ.*, 2017, **24**, 1184–1195.
- 55 N. Holler, R. Zaru, O. Micheau, M. Thome, A. Attinger, S. Valitutti, J. L. Bodmer, P. Schneider, B. Seed and J. Tschopp, Fas triggers an alternative, caspase-8-independent cell death pathway using the kinase RIP as effector molecule, *Nat. Immunol.*, 2000, **1**, 489–495.
- 56 Y. S. Cho, S. Challa, D. Moquin, R. Genga, T. D. Ray, M. Guildford and F. K. Chan, Phosphorylation-driven assembly of the RIP1-RIP3 complex regulates programmed necrosis and virus-induced inflammation, *Cell*, 2009, **137**, 1112–1123.
- 57 S. Saveljeva, S. L. Mc Laughlin, P. Vandenabeele, A. Samali and M. J. Bertrand, Endoplasmic reticulum stress induces ligand-independent TNFR1-mediated necroptosis in L929 cells, *Cell Death Dis.*, 2015, **6**, e1587.
- 58 A. L. Drummond, C. C. Weng, G. Wang, H. Chiarini-Garcia, L. Eras-Garcia and M. L. Meistrich, Effects of multiple doses of cyclophosphamide on mouse testes: accessing the

- germ cells lost, and the functional damage of stem cells, *Reprod. Toxicol.*, 2011, **32**, 395–406.
- 59 G. Q. Shen, G. C. Lu, T. J. Pan and Y. J. Xiao, [The changes of IGF-I in testis and epididymis on a rat model with oligozoospermia/azoospermia induced by cyclophosphamide], *Zhonghua Nankexue*, 2005, **11**(664–6), 669.
- 60 M. A. Dooley and R. Nair, Therapy Insight: preserving fertility in cyclophosphamide-treated patients with rheumatic disease, *Nat. Clin. Pract. Rheumatol.*, 2008, **4**, 250–257.
- 61 E. Selvakumar, C. Prahalathan, Y. Mythili and P. Varalakshmi, Protective effect of DL-alpha-lipoic acid in cyclophosphamide induced oxidative injury in rat testis, *Reprod. Toxicol.*, 2004, **19**, 163–167.
- 62 A. O. Ceribaşı, G. Türk, M. Sönmez, F. Sakin and A. Ateşşahin, Toxic effect of cyclophosphamide on sperm morphology, testicular histology and blood oxidant-antioxidant balance, and protective roles of lycopene and ellagic acid, *Basic Clin. Pharmacol. Toxicol.*, 2010, **107**, 730–736.
- 63 A. M. Abd El Tawab, N. N. Shahin and M. M. AbdelMohsen, Protective effect of *Satureja montana* extract on cyclophosphamide-induced testicular injury in rats, *Chem.-Biol. Interact.*, 2014, **224**, 196–205.
- 64 S. H. Kim, I. C. Lee, H. S. Baek, I. S. Shin, C. Moon, C. S. Bae, S. H. Kim, J. C. Kim and H. C. Kim, Mechanism for the protective effect of diallyl disulfide against cyclophosphamide acute urotoxicity in rats, *Food Chem. Toxicol.*, 2014, **64**, 110–118.
- 65 S. E. Karakas and P. Surampudi, New Biomarkers to Evaluate Hyperandrogenemic Women and Hypogonadal Men, *Adv. Clin. Chem.*, 2018, **86**, 71–125.
- 66 K. Skoracka, P. Eder, L. Łykowska-Szuber, A. Dobrowolska and I. Kreła-Kaźmierczak, Diet and Nutritional Factors in Male (In)fertility-Underestimated Factors, *J. Clin. Med.*, 2020, **9**, 1400.
- 67 J. Young, C. Xu, G. E. Papadakis, J. S. Acierno, L. Maione, J. Hietamäki, T. Raivio and N. Pitteloud, Clinical Management of Congenital Hypogonadotropic Hypogonadism, *Endocr. Rev.*, 2019, **40**, 669–710.
- 68 G. Corona, A. Pizzocaro, F. Lanfranco, A. Garolla, F. Pelliccione, L. Vignozzi, A. Ferlin, C. Foresta, E. A. Jannini, M. Maggi, *et al.*, Sperm recovery and ICSI outcomes in Klinefelter syndrome: a systematic review and meta-analysis, *Hum. Reprod. Update*, 2017, **23**, 265–275.
- 69 D. S. Guzick, J. W. Overstreet, P. Factor-Litvak, C. K. Brazil, S. T. Nakajima, C. Coutifaris, S. A. Carson, P. Cisneros, M. P. Steinkampf, J. A. Hill, *et al.*, Sperm morphology, motility, and concentration in fertile and infertile men, *N. Engl. J. Med.*, 2001, **345**, 1388–1393.
- 70 P. Jedrzejczak, G. Taszarek-Hauke, J. Hauke, L. Pawelczyk and A. J. Duleba, Prediction of spontaneous conception based on semen parameters, *Int. J. Androl.*, 2008, **31**, 499–507.